

# Reachset-Conformant System Identification

Laura Lützwow and Matthias Althoff, *Member, IEEE*

**Abstract**—Formal verification techniques play a pivotal role in ensuring the safety of complex cyber-physical systems. To transfer model-based verification results to the real world, we require that the measurements of the target system lie in the set of reachable outputs of the corresponding model, a property we refer to as reachset conformance. This paper is on automatically identifying those reachset-conformant models. While state-of-the-art reachset-conformant identification methods focus on linear state-space models, we generalize these methods to non-linear state-space models and linear and nonlinear input-output models. Furthermore, our identification framework adapts to different levels of prior knowledge on the system dynamics. In particular, we identify the set of model uncertainties for white-box models, the parameters and the set of model uncertainties for gray-box models, and entire reachset-conformant black-box models from data. For the black-box identification, we propose a new genetic programming variant, which we call conformant genetic programming. The robustness and efficacy of our framework are demonstrated in extensive numerical experiments using simulated and real-world data.

**Index Terms**—Data-defined modeling, formal safety verification, input-output models, reachability analysis, reachset conformance, set-based computing, zonotopes.

## I. INTRODUCTION

Formal verification techniques require mathematical models that describe the behavior of the target system [1]. Since no model of a cyber-physical system is completely accurate due to the inherent complexity of real-world dynamics, we include uncertainties in our models to cover the discrepancies to the target system. The automatic identification of these uncertainties alongside the nominal model is the topic of this article.

### A. Literature Overview

Classical system identification techniques aim to find the model or model parameters, which minimize some objective function, usually by making probabilistic assumptions about the uncertainty in the data and the model [2]–[5]. In many applications, however, we do not have any information about the underlying probability distributions [6]. Furthermore, to establish rigorous safety guarantees in planning and control, it is beneficial to have models with bounded uncertainties [7].

This work has been submitted to the IEEE for possible publication. Copyright may be transferred without notice, after which this version may no longer be accessible. This work was funded by the Deutsche Forschungsgemeinschaft (DFG, German Research Foundation) – SFB 1608 – under grant number 501798263.

The authors are both with the School of Computation, Information and Technology, Technical University of Munich, 85748 Garching, Germany. {laura.luetzwow@tum.de, althoff@in.tum.de}

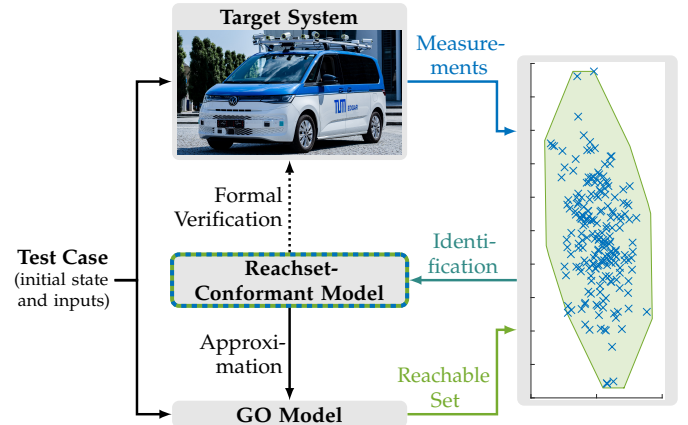


Fig. 1. Identification of a reachset-conformant model: We measure the outputs of the target system for a given initial state and input trajectory. A reachset-conformant model can be identified by adapting model parameters and the uncertainty sets until all measurements of the target system are contained in the reachable set of the model, which is computed for each initial state and input trajectory using the corresponding GO model.

Given the model structure and the bounds of an additive model uncertainty, which describes the errors between the model outputs and the measurements of the target system, the set of feasible parameters can be estimated by *set-membership methods*, also called bounded-error approaches [8]. This set of feasible parameters is overapproximated by multi-dimensional intervals [9]–[11], ellipsoids [6], or zonotopes [12]. An overapproximation with arbitrary accuracy can be obtained using unions of non-overlapping multi-dimensional intervals [13]–[15]. For linear systems, the exact parameter set can be represented by a polytope [16] if the model uncertainty is bounded by an interval, or by a matrix zonotope [17] in the case of additive zonotopic uncertainties. However, specifying the model structure and the uncertainty bounds a priori, as required for set-membership approaches, is usually a difficult task for real-world systems. If the uncertainty bounds are assumed too large, the resulting set of possible models is also too large. On the other hand, we might not find any feasible parameters if the uncertainty bounds are assumed too small.

To address these problems, techniques for *conformant model identification* have been developed [1]. These methods find optimal models and their corresponding uncertainties such that a conformance relation is established. For simplicity, we unify all uncertainties in a so-called uncertainty set. Depending on the conformance relation, different properties can be transferred from the conformant model to the system. Many publications focus on *simulation relations*, which facilitates the transfer of temporal logic properties by relating system

states [18]–[20]. Establishing a simulation relation, however, requires that the system state is observable. Less restrictive are trace conformance and reachset conformance, which only consider the output of the system. In *trace-conformant* identification, the model and uncertainty set are constructed such that the model is able to produce all output traces of the target system [21]–[23]. In most cases, this can only be done approximately, which strongly limits the usability of the resulting models for formal verification. *Reachset conformance*, on the other hand, only requires that the system output is contained in the reachable set of the model at each time step, which facilitates using simpler model structures and smaller uncertainties. As reachset conformance transfers safety properties, a reachset-conformant model suffices for formal safety verification, e.g., for collision avoidance [24] or the computation of control invariant sets [25].

Although reachset-conformant identification is a young research direction, there already exist multiple approaches to identify reachset-conformant state-space models in the literature: A given model can be made reachset-conformant by incrementally enlarging the additive uncertainty sets until all measurements are contained in the reachable set [26]. If we have estimates for the system state, we can separately compute the additive process and measurement uncertainty set as multi-dimensional intervals that contain all errors between the system states and the states predicted by the model, and between the measurements and the model outputs [27]. Given full state measurements, the reachset-conformant identification of linear models with additive, zonotopic uncertainty sets can be formulated as a convex programming problem minimizing the size of the uncertainty sets [28]. Furthermore, additive, zonotopic uncertainty sets for linear systems can be computed with a linear program that minimizes the interval norm of the resulting reachable set [29]. This method can be extended to the identification of the initial state uncertainty set and the minimization of the Frobenius norm of the reachable set [30]. The scalability of the linear program with respect to the system dimension and time horizon can be improved by using the generator representation instead of the halfspace representation of the reachable set [31].

## B. Contributions and Outline

To the best of our knowledge, there exist no publications about a) the reachset-conformant identification of arbitrary (non-additive) uncertainty sets, b) the reachset-conformant identification of input-output models such as autoregressive models with exogenous inputs (ARX models) or nonlinear autoregressive model with exogenous inputs (NARX models), and c) reachset-conformant black-box identification based entirely on data. Our work addresses these topics by proposing a general framework for reachset-conformant system identification, as visualized in Fig. 1. In particular, our contributions are as follows:

- We present a general output (GO) model and derive how the input-output behavior of state-space models and input-output models can be approximated by this model.
- We compute, for the first time, the reachable set of nonlinear input-output models using the GO model.
- Furthermore, we present a linear program for the reachset-conformant white-box identification of linear and nonlinear models, i.e., we identify the uncertainty sets such that reachset conformance is established. Thus, we are the first to estimate, possibly non-additive, uncertainty sets for input-output models and nonlinear state-space models.
- Additionally, we propose a framework for the identification of reachset-conformant models from data with little (gray-box identification) or no prior knowledge about the system dynamics (black-box identification).
- The performance and scalability of the proposed approaches is analyzed in numerical experiments for different dynamical systems and considering different levels of prior knowledge.
- We demonstrate real-world applicability by identifying a reachset-conformant vehicle model from real-world data.

This article is structured as follows: Fundamentals about zonotopes and reachset conformance and the problem statement are introduced in Sec. II. In Sec. III, we present a general approach to compute the reachable set of different model types using the novel GO model. Sec. IV deals with the reachset-conformant identification of uncertainty sets for given model dynamics. Subsequently, we extend this approach to cases where the model dynamics contain unknown parameters in Sec. V and cases where we do not have any knowledge about the model in Sec. VI. The efficacy of our approaches is demonstrated in numerical experiments in Sec. VII and Sec. VIII concludes this article.

## C. Notations

Sets are denoted by calligraphic letters, matrices by uppercase letters, and vectors and scalars by lowercase letters. Furthermore, we use  $\mathbf{1}$ ,  $\mathbf{I}$ , and  $\mathbf{0}$ , respectively, for a vector filled with ones, the identity matrix, and a matrix of zeros, where the matrix dimensions can be explicitly written in the subscript. The operation  $\text{diag}(v)$  returns a diagonal matrix with the elements of the vector  $v$  on its main diagonal,  $\text{diag}(A_1, A_2, \dots, A_n)$  represents a blockdiagonal matrix where the matrices  $A_1, A_2, \dots, A_n$  are concatenated diagonally,  $\text{diag}_n(A)$  is a blockdiagonal matrix where  $n$  copies of the matrix  $A$  are concatenated diagonally, and  $\text{vert}_n(A)$  describes the vertical concatenation of  $n$  copies of the matrix  $A$ . Additionally, we introduce the notation  $v_{0:k}$  for the vertical concatenation  $[v_0^\top \ v_1^\top \ \dots \ v_k^\top]^\top$  of the time-varying vector  $v_i \in \mathbb{R}^m$  for the time steps  $i = 0, \dots, k$ . The Jacobian of  $f(v_{0:k}): \mathbb{R}^{(k+1)m} \rightarrow \mathbb{R}^n$  with respect to the vector  $v_i$  is written as  $\nabla_{v_i} f = [\frac{\partial f}{\partial v_{i,1}} \ \dots \ \frac{\partial f}{\partial v_{i,m}}]$ , where  $v_{i,j}$  denotes the  $j$ -th element of  $v_i$ .

Let us also introduce the Minkowski sum of two sets  $S_a, S_b \subset \mathbb{R}^n$  as  $S_a \oplus S_b = \{s_a + s_b \mid s_a \in S_a, s_b \in S_b\}$ , the Cartesian product  $S_a \times S_b = \{[s_a^\top \ s_b^\top]^\top \mid s_a \in S_a, s_b \in S_b\}$ , and the linear transformation using the matrix  $A \in \mathbb{R}^{m \times n}$  as  $AS = \{As \mid s \in S\}$ . The Cartesian product  $S_0 \times S_1 \times \dots \times S_k$  of the sequence of sets  $S_i, i = 0, \dots, k$ , is denoted by  $S_{0:k}$ .

## II. PRELIMINARIES AND PROBLEM STATEMENT

We first introduce zonotopes, which is the set representation used in this work, followed by the definition of reachset conformance. Subsequently, we formulate our problem statement.

### A. Zonotopes

A zonotope is a convex set representation that is closed under Minkowski sum and linear map. The generator representation of zonotopes makes it possible to efficiently compute the aforementioned operations in high dimensions [32]:

*Definition 1 (Generator Representation of Zonotopes [33]):*

A zonotope  $\mathcal{Z} \subset \mathbb{R}^n$  can be described by its center vector  $c = \text{cen}(\mathcal{Z}) \in \mathbb{R}^n$  and its generator matrix  $G = \text{gen}(\mathcal{Z}) = [g_1 \dots g_n] \in \mathbb{R}^{n \times n}$  as

$$\mathcal{Z} = \left\{ c + \sum_{i=1}^n \lambda_i g_i \mid \lambda_i \in [-1, 1] \right\} = \langle c, G \rangle.$$

Alternatively, zonotopes can be described by their halfspace representation:

*Definition 2 (Halfspace Representation of Zonotopes [34]):*

A zonotope  $\mathcal{Z} \subset \mathbb{R}^n$  can be represented as the intersection of a finite number of halfspaces, whose normal vectors are concatenated row-wise in the matrix  $N \in \mathbb{R}^{h \times n}$  and whose offsets to the origin are stacked in the vector  $d \in \mathbb{R}^h$ :

$$\mathcal{Z} = \{x \in \mathbb{R}^n \mid Nx \leq d\}.$$

A zonotope in generator representation can be converted to its halfspace representation using [34, Thm. 7]. Generally, computations using the generator representation scale better with increasing dimension than the halfspace representation, since a zonotope with  $\eta$  generators has up to  $2 \binom{\eta}{n-1}$  halfspaces [34] and thus, the number of halfspaces  $h$  grows exponentially with the dimension  $n$ . Furthermore, the set operations Minkowski sum, Cartesian product, and linear transformation can be efficiently performed in generator representation: For two zonotopes  $\mathcal{Z}_a = \langle c_a, G_a \rangle$  and  $\mathcal{Z}_b = \langle c_b, G_b \rangle$  and the matrix  $A$ , we have  $\mathcal{Z}_a \oplus \mathcal{Z}_b = \langle c_a + c_b, [G_a \ G_b] \rangle$ ,  $\mathcal{Z}_a \times \mathcal{Z}_b = \langle [c_a^\top \ c_b^\top]^\top, \text{diag}(G_a, G_b) \rangle$ , and  $A\mathcal{Z}_a = \langle Ac_a, AG_a \rangle$ . The size of a zonotope can be evaluated using the interval norm:

*Definition 3 (Interval Norm of Zonotopes [30, Sec. 3.1]):*

The interval norm for the zonotope  $\mathcal{Z} = \langle c, G \rangle$  is defined as

$$\|\mathcal{Z}\|_I = \mathbf{1}^\top |G| \mathbf{1}.$$

### B. Reachset Conformance

As measurements are usually obtained in discrete time, we only consider discrete-time systems. Let us now introduce the output  $\tau(S, k, x_0, u_{0:k})$  at time step  $k$  of a system  $S$  starting at the state  $x_0$ , controlled by the inputs stacked in  $u_{0:k} = [u_0^\top \dots u_k^\top]^\top$ , where the input vector  $u_i$  consists of the control signals and disturbances at time step  $i$ . We consider uncertainties by assuming that the initial state  $x_0$  and inputs  $u_{0:k}$  deviate from the expected initial state  $x_{*0}$  and inputs  $u_{*0:k}$ , which we call the nominal initial state and the nominal inputs. These deviations are represented by the sets  $\Delta\mathcal{X}_0$  and

$\Delta\mathcal{U}_{0:k}$ . The nominal initial state and inputs as well as the measured outputs are collected in a test case:

*Definition 4 (Test Case):* The  $m$ -th test case consists of the nominal initial state  $x_{*0}^{(m)}$ , the nominal inputs  $u_{*0:n_k-1}^{(m)}$ , and the measured outputs

$$y_k^{(m,s)} = \tau(S, k, x_0^{(m,s)}, u_{0:k}^{(m,s)}),$$

with  $k = 0, \dots, n_k - 1$ ,  $s = 1, \dots, n_s$ , and

$$x_0^{(m,s)} \in x_{*0}^{(m)} \oplus \Delta\mathcal{X}_0^{(m)} =: \mathcal{X}_{*0}^{(m)}, \quad (1a)$$

$$u_k^{(m,s)} \in u_{*k}^{(m)} \oplus \Delta\mathcal{U}_k^{(m)} =: \mathcal{U}_{*k}^{(m)}. \quad (1b)$$

We refer to the set of reachable outputs as the reachable set, which can be formally defined as follows:

*Definition 5 (Reachable Set):* The reachable set of the system  $S$  at time  $k$  is defined as

$$\text{Reach}_k(S, m) := \left\{ \tau(S, k, x_0, u_{0:k}) \mid x_0 \in \mathcal{X}_{*0}^{(m)}, u_{0:k} \in \mathcal{U}_{*0:k}^{(m)} \right\}.$$

Subsequently, we consider a real-world system or a high-fidelity model as the target system  $S_T$ . For many applications, such as real-time verification, we need a simple model  $S_M$  that is able to approximate the behavior of  $S_T$ . To transfer safety properties from the model  $S_M$  to the target system  $S_T$ , we require reachset conformance:

*Definition 6 (Reachset Conformance [1, Sec. 3]):* System  $S_M$  is a reachset-conformant model of the target system  $S_T$  if and only if for all time steps  $k$  and all possible test cases  $m$ , the reachable set  $\text{Reach}_k(S_M, m)$  contains the reachable set  $\text{Reach}_k(S_T, m)$  of  $S_T$ :

$$S_T \text{ conf}_R S_M \Leftrightarrow \forall k, m: \text{Reach}_k(S_T, m) \subseteq \text{Reach}_k(S_M, m). \quad (2)$$

Since the reachable set does not exist for real-world systems and cannot be computed for many models [35], [36], we use the following approximations: The reachable set of the target system  $S_T$  will be approximated by sampling, where

$$\text{Reach}_k(S_T, m) = \lim_{n_s \rightarrow \infty} \left\{ y_k^{(m,s)} \mid s = 1, \dots, n_s \right\}. \quad (3)$$

As we can only consider a finite number of samples  $n_s$  in practice, reachset conformance can only be checked for the given samples but not be proven in general. Furthermore, the reachable set of the model  $S_M$  might be computed with an overapproximative reachability algorithm. Reachset conformance only requires that the algorithm computing the overapproximative reachable set  $\text{Reach}_k(S_M, m)$  for the verification is identical to that used for establishing reachset conformance.

### C. Problem Statement

We present methods for an efficient identification of reachset-conformant models from data. We assume that the uncertainties  $\Delta\mathcal{X}_0^{(m)}$  and  $\Delta\mathcal{U}_k^{(m)}$ ,  $k = 0, \dots, n_k - 1$ ,  $m =$

$1, \dots, n_m$ , of the model  $S_M$  can be represented by time-invariant zonotopes that are independent of the test case:

$$\mathcal{X}_0 = \langle c_x + \Delta c_x, G_x \text{diag}(\alpha_x) \rangle, \quad \alpha_x \in \mathbb{R}_{\geq 0}^{\eta_x}, \quad (4a)$$

$$\mathcal{U}_c = \langle c_u + \Delta c_u, G_u \text{diag}(\alpha_u) \rangle, \quad \alpha_u \in \mathbb{R}_{\geq 0}^{\eta_u}, \quad (4b)$$

where the center vectors consist of the initial estimate  $c = [c_x^\top \ c_u^\top]^\top$  and an unknown center shift  $\Delta c = [\Delta c_x^\top \ \Delta c_u^\top]^\top$ , and the generator matrices are computed from the initial estimates  $G_x \in \mathbb{R}^{n_x \times \eta_x}$  and  $G_u \in \mathbb{R}^{n_u \times \eta_u}$  and unknown scaling factors  $\alpha = [\alpha_x^\top \ \alpha_u^\top]^\top$ .

We can now formulate our problem statement of identifying reachset-conformant models, which are characterized by their input-output behavior  $\tau$  and their uncertainty sets  $\mathcal{X}_0$  and  $\mathcal{U}_c$ . To reduce conservatism, we additionally minimize a cost function that evaluates the size of the reachable sets:

*Problem 1 (Reachset-conformant Identification):*

We establish reachset conformance between the model  $S_M$ , which is parameterized by  $q$  with the uncertainty sets given in (4), and the target system  $S_T$  for the test cases  $m = 1, \dots, n_m$  by solving

$$q^* = \min_q \sum_{m=1}^{n_m} \sum_{k=0}^{n_k-1} w_k r(\text{Reach}_k(S_M(q), m)) \quad (5a)$$

$$\text{s.t.} \quad \forall k, m, s: y_k^{(m,s)} \in \text{Reach}_k(S_M(q), m), \quad (5b)$$

where the function  $r(\mathcal{S})$  evaluates the size of a set  $\mathcal{S}$ ,  $y_k^{(m,s)}$  are the measurements of the system  $S_T$ , and  $w_k \geq 0$  is a weight for time step  $k$ .

From this general problem, we derive the following sub-problems considered in this work:

*Problem 1.1 (Identification of White-Box Models):*

We solve Problem 1 with the optimization variables  $q = (\alpha, \Delta c)$ , assuming the input-output behavior  $\tau$  of the model  $S_M$  is known.

*Problem 1.2 (Identification of Gray-Box Models):*

We solve Problem 1 with the optimization variables  $q = (\alpha, \Delta c, p)$ , assuming the input-output behavior  $\tau$  of the model  $S_M$  depends on unknown model parameters  $p$ .

*Problem 1.3 (Identification of Black-Box Models):*

We solve Problem 1 with the optimization variables  $q = (\alpha, \Delta c, \tau)$ , where  $\tau$  denotes the unknown input-output behavior of the model  $S_M$ .

Estimating arbitrary model parameters  $p$  or the input-output behavior  $\tau$  in Problem 1.2 and Problem 1.3 are complex, non-linear programming problems. As no optimization techniques are guaranteed to find the global optimal solution for these problems in finite time, we will focus on efficiently finding a good local optimum that satisfies the conformance constraints.

### III. REACHABILITY ANALYSIS

In this section, we explain how to generalize reachability analysis for different model types. First, we propose a so-called general output model and compute its reachable set. These results are then used to compute the reachable set of state-space models and input-output models.

#### A. General Output Model

The general output model can be defined as follows:

*Definition 7 (General Output (GO) Model):*

The GO model  $\bar{S}_M(\bar{x}_0, \bar{u}_{0:k})$  returns a general, linear approximation of the output of the model  $S_M$  along the reference trajectory defined by  $\bar{x}_0$  and  $\bar{u}_{0:k}$ :

$$\begin{aligned} \tau(\bar{S}_M(\bar{x}_0, \bar{u}_{0:k}), k, x_0, u_{0:k}) &= \bar{y}_k + \bar{C}_k(x_0 - \bar{x}_0) \\ &\quad + \sum_{i=0}^k \bar{D}_{k,i}(u_i - \bar{u}_i). \end{aligned} \quad (6)$$

where  $\bar{y}_k$  is the reference output,  $\bar{C}_k$  is the system matrix, and  $\bar{D}_{k,i}$  are the input matrices of  $\bar{S}_M(\bar{x}_0, \bar{u}_{0:k})$ . The deviation between the output of  $\bar{S}_M(\bar{x}_0, \bar{u}_{0:k})$  and the output of  $S_M$  is described by the linearization error  $e_k$ :

$$e_k = \tau(S_M, k, x_0, u_{0:k}) - \tau(\bar{S}_M(\bar{x}_0, \bar{u}_{0:k}), k, x_0, u_{0:k}).$$

Since the GO model is linear, its exact reachable set can be computed:

*Proposition 1 (Reachable Sets of GO Models):*

The reachable set of the GO model  $\bar{S}_M(\bar{x}_0, \bar{u}_{0:k})$  with the uncertainty sets  $\mathcal{X}_{*0}^{(m)}$  and  $\mathcal{U}_{*0:k}^{(m)}$  can be computed as

$$\text{Reach}_k(\bar{S}_M(\bar{x}_0, \bar{u}_{0:k}), m) = \bar{y}_k \oplus \mathcal{Y}_{a,k}^{(m)}, \quad (7)$$

with

$$\mathcal{Y}_{a,k}^{(m)} = \bar{C}_k(\mathcal{X}_{*0}^{(m)} - \bar{x}_0) \oplus \bigoplus_{i=0}^k \bar{D}_{k,i}(\mathcal{U}_{*i}^{(m)} - \bar{u}_i). \quad (8)$$

*Proof:* Eq. (7) and (8) can be obtained by a set-based evaluation of (6) with the uncertainties  $x_0 \in \mathcal{X}_{*0}$  and  $u_{0:k} \in \mathcal{U}_{*0:k}$ . Since the uncertain initial state and all uncertain input variables only occur once in the GO model and are assumed to be mutually independent, we can compute  $\mathcal{Y}_{a,k}$  with (8) without encountering the dependency effect, which would introduce additional conservatism [37, Sec. 2.2.3]. ■

#### B. Other Model Types

Using the GO model, we can simplify reachability analysis for other model types as follows:

*Theorem 1 (Reachable Set of Arbitrary Models):* The reachable set of a model  $S_M$  with the uncertainty sets  $\mathcal{X}_{*0}^{(m)}$  and  $\mathcal{U}_{*0:k}^{(m)}$  can be overapproximated as

$$\text{Reach}_k(S_M, m) = \text{Reach}_k(\bar{S}_M(\bar{x}_0, \bar{u}_{0:k}), m) \oplus \hat{\mathcal{E}}_k, \quad (9)$$

where  $\text{Reach}_k(\bar{S}_M(\bar{x}_0, \bar{u}_{0:k}), m)$  can be computed using (7) and the set  $\hat{\mathcal{E}}_k$  encloses all linearization errors  $e_k$ .

*Proof:* Using Def. 7, the output of  $S_M$  can be written as

$$\tau(S_M, k, x_0, u_{0:k}) = \tau(\bar{S}_M(\bar{x}_0, \bar{u}_{0:k}), k, x_0, u_{0:k}) + e_k.$$

A set-based evaluation leads to (9), where the set of linearization errors  $e_k$  is enclosed by  $\hat{\mathcal{E}}_k$ . ■

Note that the size of the linearization errors depends on the parametrization of the GO model. To obtain small linearization errors, we compute the GO model from a first-order Taylor

series expansion of the output of the model  $S_M$  along the reference trajectory, where we set  $\bar{x}_0$  and  $\bar{u}_{0:k}$  to the expected centers of the uncertainty sets  $\mathcal{X}_{*0}^{(m)}$  and  $\mathcal{U}_{*0:k}^{(m)}$  for each test case  $m$ , i.e.,

$$\bar{x}_0 = x_{*0}^{(m)} + c_x, \quad (10a)$$

$$\bar{u}_i = u_{*i}^{(m)} + c_u, \quad i = 0, \dots, k. \quad (10b)$$

Thus, we obtain the following reachability approaches for different model types:

1) *State-Space Models*: A popular model type, which is especially used in control applications, is the state-space model. In the general nonlinear case, it can be described by:

$$x_{k+1} = f(x_k, u_k) \quad (11a)$$

$$y_k = g(x_k, u_k). \quad (11b)$$

*Corollary 1 (Reachability of State-Space Models)*: The reachable set of the state-space model in (11) can be computed using Thm. 1. The reference output is  $\bar{y}_k = g(\bar{x}_k, \bar{u}_k)$ , which is obtained from simulating (11) along the reference trajectory, and the system matrix, the input matrices, and the set enclosing the linearization errors are

$$\begin{aligned} \bar{C}_k &= C_k \prod_{l=1}^k A_{k-l}, \\ \bar{D}_{k,i} &= \begin{cases} C_k \left( \prod_{l=1}^{k-i-1} A_{k-l} \right) B_i & 0 \leq i < k, \\ D_k & i = k, \end{cases} \\ \hat{\mathcal{E}}_k &= C_k \bigoplus_{j=0}^{k-1} \left( \prod_{l=1}^{k-j-1} A_{k-l} \right) \hat{\mathcal{L}}_{x,j} \oplus \hat{\mathcal{L}}_{y,k}, \end{aligned}$$

where  $\hat{\mathcal{L}}_{x,j}$  and  $\hat{\mathcal{L}}_{y,k}$  can be computed as in [38, Sec. 3.1] and

$$\begin{aligned} A_k &= \nabla_{x_k} f(x_k, u_k)|_{\bar{x}_k, \bar{u}_k}, \quad B_k = \nabla_{u_k} f(x_k, u_k)|_{\bar{x}_k, \bar{u}_k}, \\ C_k &= \nabla_{x_k} g(x_k, u_k)|_{\bar{x}_k, \bar{u}_k}, \quad D_k = \nabla_{u_k} g(x_k, u_k)|_{\bar{x}_k, \bar{u}_k}. \end{aligned}$$

*Proof*: Applying a Taylor expansion of order  $\kappa$  with Lagrange remainder to (11) along the reference trajectory, we obtain

$$x_{k+1} = f(\bar{x}_k, \bar{u}_k) + A_k(x_k - \bar{x}_k) + B_k(u_k - \bar{u}_k) + l_{x,k} \quad (12)$$

$$y_k = g(\bar{x}_k, \bar{u}_k) + C_k(x_k - \bar{x}_k) + D_k(u_k - \bar{u}_k) + l_{y,k}, \quad (13)$$

where  $l_{x,k} \in \mathcal{L}_{x,k}$  and  $l_{y,k} \in \mathcal{L}_{y,k}$  contain the Taylor terms from order two up to order  $\kappa$  and the Lagrange remainders [38]. Recursively inserting (12) in (13) leads to the GO model defined by the formulas above with

$$e_k = C_k \sum_{j=0}^{k-1} \left( \prod_{l=1}^{k-j-1} A_{k-l} \right) l_{x,j} + l_{y,k}.$$

The set  $\hat{\mathcal{E}}_k$  enclosing the linearization errors is computed by a set-based evaluation of  $e_k$  using the overapproximations  $\hat{\mathcal{L}}_{x,j} \supseteq \mathcal{L}_{x,j}$  and  $\hat{\mathcal{L}}_{y,k} \supseteq \mathcal{L}_{y,k}$  from [38, Sec. 3.1]. ■

For the special case of linear state-space models, we have  $\hat{\mathcal{E}}_k = \mathbf{0}$ .

To compute the reachable set, we require some estimate for the initial state  $x_{*0}$ , which is often not directly measurable for state-space models. In that case, guaranteed state estimation [39] is required, which introduces additional uncertainties compared to equivalent input-output models that are directly initialized with the measurements [40]. Thus, input-output models represent an important model class for data-driven system identification.

2) *Input-Output Models*: A general input-output model is the NARX model, which computes the current output from previous outputs and the current and previous inputs. It can be described by

$$y_k = f(y_{k-n_p:k-1}, u_{k-n_p:k}). \quad (14)$$

If the function  $f$  is linear in  $y_{k-n_p:k-1}$  and  $u_{k-n_p:k}$ , we call the model ARX model.

By combining a Taylor expansion with the reformulation from [40, Thm. 1], we obtain the following formulas to compute the reachable set of (14):

*Corollary 2 (Reachability of Input-Output Models)*: The reachable set of the input-output model in (14) can be computed using Thm. 1, where  $k \geq n_p$ . The reference output is  $\bar{y}_k = f(\bar{y}_{k-n_p:k-1}, \bar{u}_{k-n_p:k})$ , which is obtained by simulating (14) along the reference trajectory, and the system matrix, the input matrices, and the set enclosing the linearization errors are

$$\begin{aligned} \bar{C}_k &= E \prod_{l=0}^{k-n_p} A_{\text{ext},k-l}, \\ \bar{D}_{k,i} &= E \sum_{j=0}^{k-n_p} \left( \prod_{l=0}^{j-1} A_{\text{ext},k-l} \right) B_{\text{ext},k-j,k-i-j}, \\ \hat{\mathcal{E}}_k &= E \bigoplus_{j=0}^{k-n_p} \left( \prod_{l=0}^{j-1} A_{\text{ext},k-l} \right) E^\top \hat{\mathcal{L}}_{k-j}, \end{aligned}$$

where  $\hat{\mathcal{L}}_k$  can be computed analogously to [38, Sec. 3.1] and

$$\begin{aligned} E &= \begin{bmatrix} \mathbf{0}_{n_y \times (n_p-1)n_y} & \mathbf{I}_{n_y} \end{bmatrix}, \\ A_{\text{ext},k} &= \begin{bmatrix} \mathbf{0}_{(n_p-1)n_y \times n_y} & \mathbf{I}_{(n_p-1)n_y} \\ A_{k,n_p} & [A_{k,n_p-1} \dots A_{k,1}] \end{bmatrix}, \\ B_{\text{ext},k,i} &= \begin{bmatrix} \mathbf{0}_{(n_p-1)n_y \times n_u} \\ B_{k,i} \end{bmatrix}, \\ A_{k,i} &= \nabla_{y_{k-i}} f(y_{k-n_p:k-1}, u_{k-n_p:k})|_{\bar{y}_{k-n_p:k-1}, \bar{u}_{k-n_p:k}}, \\ B_{k,i} &= \nabla_{u_{k-i}} f(y_{k-n_p:k-1}, u_{k-n_p:k})|_{\bar{y}_{k-n_p:k-1}, \bar{u}_{k-n_p:k}}, \end{aligned}$$

The initial state consists of the initial measurements:

$$x_0 = [y_0^\top \ y_1^\top \ \dots \ y_{n_p-1}^\top]^\top. \quad (15)$$

*Proof*: The output of the NARX model can be approximated by a Taylor series of order  $\kappa$  along the reference trajectory defined by  $\bar{x}_0 = [\bar{y}_0^\top \ \bar{y}_1^\top \ \dots \ \bar{y}_{n_p-1}^\top]^\top$  and  $\bar{u}_{0:k}$ :

$$\begin{aligned} y_k &= f(\bar{y}_{k-n_p:k-1}, \bar{u}_{k-n_p:k}) + \sum_{i=1}^{n_p} A_{k,i} (y_{k-i} - \bar{y}_{k-i}) \\ &+ \sum_{i=0}^{n_p} B_{k,i} (u_{k-i} - \bar{u}_{k-i}) + l_k, \end{aligned}$$

where  $l_k \in \mathcal{L}_k$  contains the Taylor terms from order two up to order  $\kappa$  and the Lagrange remainder [38]. A reformulation analog to [40, Thm. 1] with the initial state as in (15) results in the GO model defined by the formulas above with

$$e_k = E \sum_{j=0}^{k-n_p} \left( \prod_{l=0}^{j-1} A_{\text{ext},k-l} \right) E^\top l_{k-j}.$$

A set-based evaluation of  $e_k$  leads to the set  $\widehat{\mathcal{E}}_k$  using the overapproximation  $\widehat{\mathcal{L}}_k \supseteq \mathcal{L}_k$  from [38, Sec. 3.1]. ■

For the special case of ARX models, we have  $\widehat{\mathcal{E}}_k = \mathbf{0}$ .

#### IV. IDENTIFICATION OF WHITE-BOX MODELS

This section describes the general framework to identify the uncertainty sets that make a model reachset-conformant (Problem 1.1). For linear models and the zonotopic uncertainty sets in (4), reachset-conformant scaling factors  $\alpha$  and center vector shifts  $\Delta c$  can be identified with linear programming [31]. This approach can be generalized to a nonlinear model by computing its reachable set using Thm. 1 for each test case  $m$  and the reference trajectories in (10). To formulate the white-box identification problem as a linear program, we require the following lemmas:

*Lemma 1 (Set of Output Deviations):* The center vector and generators of the set of output deviations  $\mathcal{Y}_{a,k} = \langle \text{cen}(\mathcal{Y}_{a,k}), \text{gen}(\mathcal{Y}_{a,k}) \rangle$  are

$$\text{cen}(\mathcal{Y}_{a,k}) = \bar{C}_k \Delta c_x + \sum_{j=0}^k \bar{D}_{k,j} \Delta c_u, \quad (16a)$$

$$\text{gen}(\mathcal{Y}_{a,k}) = \text{gen}'(\mathcal{Y}_{a,k}) \text{diag} \left( [\alpha_x^\top \quad \alpha_u^\top \quad \dots \quad \alpha_u^\top]^\top \right), \quad (16b)$$

$$\text{gen}'(\mathcal{Y}_{a,k}) = [\bar{C}_k G_x \quad \bar{D}_{k,0} G_u \quad \dots \quad \bar{D}_{k,k} G_u]. \quad (16c)$$

*Proof:* By inserting the uncertain states  $\mathcal{X}_{*0}$  and inputs  $\mathcal{U}_{*i}$ ,  $i = 0, \dots, k$ , from (1) with the uncertainty sets from (4) and the reference signals from (10) in (8), we obtain the generator representation of  $\mathcal{Y}_{a,k}$  as given in (16). ■

*Lemma 2 (Halfspace Constraints):* The containment constraint  $\forall m, s, k: y_k^{(m,s)} \in \bar{y}_k^{(m)} \oplus \mathcal{Y}_{a,k}^{(m)}$ , is equivalent to

$$\forall k, m: y_{k,\max}^{(m)} \leq P_{\alpha,k}^{(m)} \alpha + P_{c,k}^{(m)} \Delta c, \quad (17)$$

with  $\alpha \geq \mathbf{0}$  and

$$y_{k,\max}^{(m)} = \max_s \left( N_k^{(m)} y_{a,k}^{(m,s)} \right),$$

$$P_{\alpha,k}^{(m)} = \left[ |N_k^{(m)} \bar{C}_k^{(m)} G_x| \quad \sum_{j=0}^k |N_k^{(m)} \bar{D}_{k,j}^{(m)} G_u| \right],$$

$$P_{c,k}^{(m)} = \left[ N_k^{(m)} \bar{C}_k^{(m)} \quad N_k^{(m)} \sum_{j=0}^k \bar{D}_{k,j}^{(m)} \right].$$

The rows of  $N_k^{(m)}$  are the normal vectors of the halfspace representation of  $\mathcal{Y}_{a,k}^{(m)}$ , which can be obtained using [34, Thm. 7].

*Proof:* By subtracting  $\bar{y}_k^{(m)}$  on both sides, we can write the constraint  $y_k^{(m,s)} \in \bar{y}_k^{(m)} \oplus \mathcal{Y}_{a,k}^{(m)}$  as  $y_{a,k}^{(m,s)} \in \mathcal{Y}_{a,k}^{(m)}$ . With the halfspace representation of  $\mathcal{Y}_{a,k}^{(m)}$ , where  $\mathcal{Y}_{a,k}^{(m)}$  can be computed with (16), this constraint can be enforced for each test case  $m$  analogously to [31, Thm. 2]. ■

*Lemma 3 (Generator Constraints):* The containment constraint  $\forall m, s, k: y_k^{(m,s)} \in \bar{y}_k^{(m)} \oplus \mathcal{Y}_{a,k}^{(m)}$  is equivalent to

$$\begin{bmatrix} \mathbf{0} \\ \mathbf{0} \end{bmatrix} \leq \begin{bmatrix} R_\alpha \alpha + \beta \\ R_\alpha \alpha - \beta \end{bmatrix}, \quad (18a)$$

$$\tilde{y}_a = Q_c \Delta c + Q_\beta \beta, \quad (18b)$$

with  $\alpha \geq \mathbf{0}$ , the vector of stacked measurement deviations

$$\tilde{y}_a = \left[ \tilde{y}_a^{(1)\top} \quad \dots \quad \tilde{y}_a^{(n_m)\top} \right]^\top,$$

$$\tilde{y}_a^{(m)} = \left[ \tilde{y}_{a,0:k}^{(m,1)\top} \quad \dots \quad \tilde{y}_{a,0:k}^{(m,n_s)\top} \right]^\top,$$

and the auxiliary optimization variable  $\beta \in \mathbb{R}^{n_\beta}$ ,  $n_\beta = n_m n_s \sum_{k=0}^{n_k-1} (\eta_x + (k+1)\eta_u)$ . The constraint matrices are

$$Q_c = \left[ Q_c^{(1)\top} \quad \dots \quad Q_c^{(n_m)\top} \right]^\top,$$

$$Q_c^{(m)} = \text{vert}_{n_s} \left( \begin{bmatrix} \bar{C}_0^{(m)} & \sum_{j=0}^0 \bar{D}_{0,j}^{(m)} \\ \vdots & \vdots \\ \bar{C}_{n_k-1}^{(m)} & \sum_{j=0}^{n_k-1} \bar{D}_{n_k-1,j}^{(m)} \end{bmatrix} \right),$$

$$Q_\beta = \text{diag} \left( Q_\beta^{(1)}, \dots, Q_\beta^{(n_m)} \right),$$

$$Q_\beta^{(m)} = \text{diag}_{n_s} \left( \text{gen}'(\mathcal{Y}_{a,0}^{(m)}), \dots, \text{gen}'(\mathcal{Y}_{a,n_k-1}^{(m)}) \right),$$

$$R_\alpha = \text{vert}_{n_m n_s} \left( \begin{bmatrix} R_{\alpha,0} \\ \vdots \\ R_{\alpha,n_k-1} \end{bmatrix} \right),$$

$$R_{\alpha,k} = \begin{bmatrix} \mathbf{I}_{\eta_x} & \mathbf{0}_{\eta_x \times \eta_u} \\ \mathbf{0}_{(k+1)\eta_u \times \eta_x} & \text{vert}_{k+1}(\mathbf{I}_{\eta_u}) \end{bmatrix},$$

with  $\text{gen}'(\mathcal{Y}_{a,k}^{(m)})$  from (16c).

*Proof:* We can write the constraint  $y_k^{(m,s)} \in \bar{y}_k^{(m)} \oplus \mathcal{Y}_{a,k}^{(m)}$  as  $y_{a,k}^{(m,s)} \in \mathcal{Y}_{a,k}^{(m)}$  after subtracting  $\bar{y}_k^{(m)}$  on both sides. This constraint can be enforced via the generator representation of  $\mathcal{Y}_{a,k}^{(m)}$  analogously to [31, Thm. 3], where  $\mathcal{Y}_{a,k}^{(m)}$  can be computed with (16). This leads to

$$y_{a,k}^{(m,s)} \in \mathcal{Y}_{a,k}^{(m)}$$

$$\Leftrightarrow \exists \beta_k^{(m,s)} \in \mathbb{R}^{\eta_x + (k+1)\eta_u}:$$

$$|\beta_k^{(m,s)}| \leq [\alpha_x^\top \quad \alpha_u^\top \quad \dots \quad \alpha_u^\top]^\top, \quad (20a)$$

$$y_{a,k}^{(m,s)} = \left[ \bar{C}_k^{(m)} \quad \sum_{j=0}^k \bar{D}_{k,j}^{(m)} \quad \text{gen}'(\mathcal{Y}_{a,k}^{(m)}) \right]$$

$$\left[ \Delta c_x^\top \quad \Delta c_u^\top \quad \beta_k^{(m,s)\top} \right]^\top, \quad (20b)$$

where  $\beta_k^{(m,s)} := \text{diag}([\alpha_x^\top \quad \alpha_u^\top \quad \dots \quad \alpha_u^\top]^\top) \lambda_k^{(m,s)}$ . Stacking

the vectors  $\beta_k^{(m,s)}$  for all measurements and time steps, i.e.,

$$\begin{aligned}\beta &= [\beta^{(1)\top} \quad \dots \quad \beta^{(n_m)\top}]^\top, \\ \beta^{(m)} &= [\beta^{(m,1)\top} \quad \dots \quad \beta^{(m,n_s)\top}]^\top, \\ \beta^{(m,s)} &= [\beta_0^{(m,s)\top} \quad \dots \quad \beta_{n_k-1}^{(m,s)\top}]^\top,\end{aligned}$$

results in the constraints (18a) and (18b). ■

Lemma 2 and Lemma 3 both transform the containment constraint  $y_k^{(m,s)} \in \bar{y}_k^{(m)} \oplus \mathcal{Y}_{a,k}^{(m)}$  to constraints that are linear in  $\alpha$  and  $\Delta c$ . Both lemmas can be used interchangeably in the following optimization problem:

*Theorem 2 (White-Box Identification of Uncertainty Sets):*

Problem 1.1 can be solved by the linear program

$$\arg \min_{\alpha, \Delta c, \beta} \gamma \alpha \quad (21a)$$

$$\text{s.t.} \quad \text{constraint (17) or (18)}, \quad (21b)$$

$$\alpha \geq \mathbf{0}, \quad (21c)$$

$$B_c \Delta c = \mathbf{0}, \quad (21d)$$

with

$$\gamma = \sum_{m=1}^{n_m} \sum_{k=0}^{n_k-1} w_k \mathbf{1}^\top \left[ |\bar{C}_k^{(m)} G_x| \quad \sum_{j=0}^k |\bar{D}_{k,j}^{(m)} G_u| \right], \quad (22)$$

$$B_c = \begin{cases} \mathbf{0} & \text{if } S_M \text{ is linear,} \\ \mathbf{I} & \text{otherwise.} \end{cases} \quad (23)$$

The optimization variable  $\beta$  only has to be included when using the generator constraint (18).

*Proof:* If the sets of linearization errors  $\hat{\mathcal{E}}_k$  used in (9) contain the zero vectors, i.e.,  $\mathbf{0} \in \hat{\mathcal{E}}_k$ ,  $k = 0, \dots, n_k - 1$ , then  $\text{Reach}_k(S_M, m)$  is underapproximated by  $\text{Reach}_k(\bar{S}_M(\bar{x}_0, \bar{u}_{0:k}), m)$ , which can be computed using (7). By using this underapproximation and defining the function

$$r(\text{Reach}_k(S_M, m)) = \|\text{Reach}_k(\bar{S}_M(\bar{x}_0, \bar{u}_{0:k}), m)\|_I,$$

Problem 1.1 can be simplified to

$$\arg \min_{\alpha, \Delta c} \sum_{m=1}^{n_m} \sum_{k=0}^{n_k-1} w_k \|\bar{y}_k^{(m)} \oplus \mathcal{Y}_{a,k}^{(m)}\|_I \quad (24a)$$

$$\text{s.t.} \quad \forall k, m, s: y_k^{(m,s)} \in \bar{y}_k^{(m)} \oplus \mathcal{Y}_{a,k}^{(m)}. \quad (24b)$$

Feasible solutions to this optimization problem are guaranteed to lead to reachset-conformant models since the satisfaction of the more conservative constraint (24b) implies the satisfaction of (5b). By inserting (16b) into Def. 3 and under the constraint  $\alpha \geq \mathbf{0}$ , we obtain the linear cost in (21a) from (24a) analogously to [31, Lem. 1]. According to Lemma 2 and Lemma 3, (24b) can be expressed with the linear constraints given in (21b) and (21c).

The requirement  $\mathbf{0} \in \hat{\mathcal{E}}_k$  is trivially fulfilled for linear systems. For nonlinear systems, this condition is satisfied by Thm. 1 and many state-of-the-art reachability algorithms such as [38] if the linearization point is contained in the initial state and input sets, i.e.,  $\bar{x}_0 \in \mathcal{X}_{*0}$  and  $\bar{u}_{0:k} \in \mathcal{U}_{*0:k}$ . Since we cannot optimize  $\bar{x}_0$  and  $\bar{u}_{0:k}$  with the linear program due to the nonlinear influence on the system matrices  $\bar{C}_k$  and  $\bar{D}_{k,j}$ ,

---

### Algorithm 1 GraySim.

---

**Inputs:**

$D_C$  Conformance test cases  
 $p$  Initial estimate for the model parameters  
 $\tau(\cdot)$  Input-output behavior of model

**Outputs:**

$p^*$  Optimized model parameters  
 $\alpha^*$  Reachset-conformant scaling factors  
 $\Delta c^*$  Reachset-conformant center shifts

---

```

1: while NLP solver has not terminated do
2:    $\alpha^* \leftarrow \text{White}(D_C, \tau(p))$ 
3:    $\ell \leftarrow (25)$  using  $\alpha^*, D_C, \tau(p)$ 
4:    $p \leftarrow$  next NLP-iteration to minimize  $\ell$ 
5: end while
6:  $p^* \leftarrow p$ 
7:  $\alpha^*, \Delta c^* \leftarrow \text{White}(D_C, \tau(p^*))$ 

```

---

we also do not update the center vectors of  $\mathcal{X}_{*0}$  and  $\mathcal{U}_{*0:k}$  for nonlinear systems by setting  $\Delta c$  to zero with (21d) to ensure this containment. ■

To identify the center vectors for nonlinear models, we can consider  $c$  as a part of the unknown model parameters  $p$  and use the methods presented in the next section. Furthermore, we will refer to the optimal cost obtained with the linear program in Thm. 2 as conformance cost  $\ell$ , i.e.,

$$\ell = \gamma \alpha^*, \quad (25)$$

where  $\gamma$  is computed with (22) and  $\alpha^*$  are optimal scaling factors resulting from the linear program in Thm. 2.

## V. IDENTIFICATION OF GRAY-BOX MODELS

In this section, we extend the uncertainty identification approach from Thm. 2 to the reachset-conformant identification of gray-box models (Problem 1.2). First, we describe an algorithm that integrates the linear program from Sec. IV in a nonlinear program to simultaneously identify the uncertainty sets and the unknown model parameters. As an alternative with lower computational complexity, we present a sequential identification approach, which identifies the model parameters prior to the uncertainty estimation.

The uncertainty sets and unknown model parameters  $p$  can be simultaneously identified with the approach proposed in [41, Sec. III-B], termed `GraySim`. The general procedure is provided in Alg. 1. The function `White` returns optimal scaling factors  $\alpha^*$  and center shifts  $\Delta c^*$  for the uncertainty sets  $\mathcal{X}_0$  and  $\mathcal{U}_c$  by solving the linear program in Thm. 2. The outer nonlinear program uses the conformance cost  $\ell$  of the model  $S_M(p)$  to optimize the parameters  $p$  until the solver converges or exceeds a maximum number of iterations. While we do not have any guarantees for finding the globally optimal parameters, we can ensure that the final model is reachset-conformant by computing the scaling factors  $\alpha^*$  and center shifts  $\Delta c^*$  with `White` for the final parameters  $p^*$ .

Solving the linear program `White` at each iteration of the NLP, as proposed in [41], leads to a high computational

**Algorithm 2** GraySeq.**Inputs:**

$D_C$  Conformance test cases  
 $p$  Initial estimate for the model parameters  
 $\tau(\cdot)$  Input-output behavior of model

**Outputs:**

$p^*$  Optimized model parameters  
 $\alpha^*$  Reachset-conformant scaling factors  
 $\Delta c^*$  Reachset-conformant center shifts

```

1: while NLP solver has not terminated do
2:    $\hat{\ell}_U \leftarrow$  (26) using  $D_C, \tau(p), \Delta c$ 
3:    $p, \Delta c \leftarrow$  next NLP-iteration to minimize  $\hat{\ell}_U$ 
4: end while
5:  $p^* \leftarrow p$ 
6:  $\alpha^*, \Delta c^* \leftarrow$  White( $D_C, \tau(p^*)$ )

```

complexity. Thus, we propose Alg. 2, termed GraySeq, resulting in shorter computation times. First, we identify model parameters  $p^*$  and center shifts  $\Delta c^*$  by minimizing an approximation  $\hat{\ell}$  of the conformance cost  $\ell$ , which is independent of the scaling factors  $\alpha$ . Next, we apply the white-box identification algorithm White on the resulting model to compute the uncertainty sets.

We propose to use the following cost function for the estimation of the parameters  $p$ :

*Proposition 2 (Underapproximative Cost Function):*

The conformance cost computed with (25) can be underapproximated by

$$\hat{\ell}_U = \sum_{m=1}^{n_m} \sum_{k=0}^{n_k-1} w_k \mathbf{1}^\top \max_s |y_{a,k}^{(m,s)} - \hat{y}_{a,k}^{(m)}|, \quad (26)$$

with

$$\hat{y}_{a,k}^{(m)} = \begin{cases} \begin{bmatrix} \bar{C}_k^{(m)} & \sum_{j=0}^k \bar{D}_{k,j}^{(m)} \end{bmatrix} \Delta c & \text{if } S_M \text{ is linear,} \\ \mathbf{0} & \text{else.} \end{cases}$$

*Proof:* From the conformance constraints in generator representation in (20), we know  $|\beta_k^{(m,s)}| \leq \alpha_k^*$  with  $\alpha_k^* := [\alpha_x^* \alpha_u^* \dots \alpha_u^*]^\top$  and

$$y_{a,k}^{(m,s)} - \bar{C}_k^{(m)} \Delta c_x - \sum_{j=0}^k \bar{D}_{k,j}^{(m)} \Delta c_u = \text{gen}'(\mathcal{Y}_{a,k}^{(m)}) \beta_k^{(m,s)}.$$

By taking the absolute value of both sides, we obtain

$$\begin{aligned} |y_{a,k}^{(m,s)} - \bar{C}_k^{(m)} \Delta c_x - \sum_{j=0}^k \bar{D}_{k,j}^{(m)} \Delta c_u| &= |\text{gen}'(\mathcal{Y}_{a,k}^{(m)}) \beta_k^{(m,s)}| \\ &\leq |\text{gen}'(\mathcal{Y}_{a,k}^{(m)})| |\beta_k^{(m,s)}| \\ &\leq |\text{gen}'(\mathcal{Y}_{a,k}^{(m)})| \alpha_k^*. \end{aligned}$$

As this has to hold for all  $s$ , we can take the maximum over  $s$ , resulting in

$$\max_s |y_{a,k}^{(m,s)} - \bar{C}_k^{(m)} \Delta c_x - \sum_{j=0}^k \bar{D}_{k,j}^{(m)} \Delta c_u| \leq |\text{gen}'(\mathcal{Y}_{a,k}^{(m)})| \alpha_k^*.$$

At the same time, the conformance cost can be formulated as

$$\ell = \sum_{m=1}^{n_m} \sum_{k=0}^{n_k-1} w_k \mathbf{1}^\top |\text{gen}'(\mathcal{Y}_{a,k}^{(m)})| \alpha_k^*.$$

Combining the last two formulas and considering constraint (21d) leads to the underapproximation  $\hat{\ell}_U \leq \gamma \alpha^*$ . ■

Although we do not have any guarantees on the closeness of the conformance cost  $\ell$  and the underapproximation  $\hat{\ell}_U$ , this cost function works well in practice as demonstrated in Sec. VII. Alternatively, we can use the least-squares cost function

$$\hat{\ell}_{LS} = \sum_{m=1}^{n_m} \sum_{k=0}^{n_k-1} w_k \mathbf{1}^\top \sum_{s=1}^{n_s} \left( y_{a,k}^{(m,s)} - \hat{y}_{a,k}^{(m)} \right)^2. \quad (27)$$

This cost function decreases the computation time even more, but the results are more vulnerable to not centrally distributed uncertainties compared to using cost functions that consider only the maximum errors. A detailed analysis of the accuracy and computation times is presented in Sec. VII-B.

## VI. IDENTIFICATION OF BLACK-BOX MODELS

For the black-box identification of reachset-conformant models (Problem 1.3), we propose a sequential approach that first identifies a model followed by the computation of the uncertainty sets using the methods from Sec. IV. As we do not assume any knowledge about the system state, we use NARX models and genetic programming in this work to approximate the system dynamics. However, other model types and black-box identification methods, such as the training of neural networks [42]–[45], can be used similarly.

Genetic programming is a global optimization technique that iteratively evolves a population of symbolic functions or entire computer programs [46]. The evolution is driven by the need to maximize a fitness function mimicking the Darwinian principle of survival of the fittest. When using genetic programming for black-box system identification [47], the evolved population consists of dynamical models with different nonlinearities, which are randomly initialized at the beginning of the evolution process. The fitness function evaluates the fit of each model to the training data. Models with a higher fitness value have a higher chance of being entirely copied or of sending model parts into the next population generation via the genetic operators crossover, mutation, and replication. The evolution process is terminated if a fitness threshold is exceeded or the maximum number of generations is reached.

As some of the models identified with genetic programming might lead to large reachable sets, even though we observed small prediction errors in the training process, we propose a new genetic programming variant termed *conformant genetic programming*. Inherent model dynamics that were not observable for the test cases in the training dataset could result in exploding reachable sets. For example, we might have a division by a near-zero number in the output equation for a particular input trajectory, which would lead to large outputs. The probability that this input trajectory is contained in the



training data is small, but the probability is significantly higher when considering whole input sets. Thus, it is advantageous to consider the conformance cost in (25), which describes the size of the reachable set for a conformant model, in the training process. However, since the computation of the conformance cost requires the solution of the linear program in Thm. 2, this cost leads to a significantly higher computational complexity than a least-squares cost function like (27) and can only be evaluated for small test suites in reasonable computation time. Hence, we propose the approach described in Alg. 3, where we first minimize a least-squares cost function, followed by a few iterations of minimizing the conformance cost. We use the following functions in the algorithm:

- **Initialize**, which randomly creates  $n_\tau$  models with different input-output behavior [48, Sec. 3.2],
- **Evolve**, which implements the evolution process based on the fitness values of the models [48, Sec. 3.2] (if all fitness values are equal to zero, as in the first iteration, the initial models are returned),
- **Best**, which returns the models with the highest fitness values, where the last argument specifies the number of returned models, and
- **White**, which estimates reachset-conformant scaling factors and center shifts by solving the linear program from Thm. 2.

First, we randomly initialize a population of  $n_\tau$  models in Line 1 and set the initial fitness values for each model to zero in Line 2. For the first  $n_g$  generations, we use the negative least-squares cost function as the fitness function to efficiently find good model candidates (see Line 3 to Line 9). From the optimized model candidates, we choose the  $\tilde{n}_\tau$  models with the highest fitness values in Line 10. In the second part of the algorithm, we optimize the obtained models by minimizing the conformance cost for the second training dataset  $D_{T2}$ . To keep the computational complexity small, we split the dataset  $D_{T2}$  into the subdatasets  $D_{T2,l}$ ,  $l = 1, \dots, n_v$ , and compute the conformance cost for each model and subdataset separately in Line 16. The fitness value is computed in Line 18 as the sum of the negative conformance costs of all subdatasets. Having reached the maximum number of generations  $\tilde{n}_g$ , we choose the model with the highest fitness in Line 21 and compute reachset-conformant scaling factors and center shifts for the test cases in  $D_C$  with Thm. 2 in Line 22.

## VII. NUMERICAL EXPERIMENTS

First, we evaluate the scalability of our white-box identification approach. Next, we analyze the general performance of the proposed white-, gray-, and black-box identification methods for different model types and compare them to baseline methods. Finally, we identify a reachset-conformant vehicle model from real-world measurements.

All methods are implemented in the MATLAB toolbox CORA [49] and are evaluated on an AMD EPYC 7763 processor with 2TB RAM and NVIDIA A100 40GB GPU. Continuous-time models will be discretized for the identification using the forward Euler method.

---

### Algorithm 3 BLaCkCGP.

---

**Inputs:**

- $D_{T1}$  Training test cases for step 1
- $D_{T2}$  Training test cases for step 2
- $D_C$  Conformance test cases

**Outputs:**

- $\tau^*$  Identified input-output behavior
  - $\alpha^*$  Reachset-conformant scaling factors
  - $\Delta c^*$  Reachset-conformant center shifts
- 

*Step 1: Minimize least-squares cost*

- 1:  $\{\tau_1, \dots, \tau_{n_\tau}\} \leftarrow \text{Initialize}$
- 2:  $\{\ell_1, \dots, \ell_{n_\tau}\} \leftarrow 0$
- 3: **for**  $i = \{1, \dots, n_g\}$  **do**
- 4:  $\{\tau_1, \dots, \tau_{n_\tau}\} \leftarrow \text{Evolve}((\tau_1, \ell_1), \dots, (\tau_{n_\tau}, \ell_{n_\tau}))$
- 5: **for**  $j = \{1, \dots, n_\tau\}$  **do**
- 6:  $\ell_{LS} \leftarrow (27)$  using  $D_{T1}, \tau_j$
- 7:  $\ell_j \leftarrow -\ell_{LS}$
- 8: **end for**
- 9: **end for**
- 10:  $\{\tau_1, \dots, \tau_{\tilde{n}_\tau}\} \leftarrow \text{Best}((\tau_1, \ell_1), \dots, (\tau_{n_\tau}, \ell_{n_\tau}), \tilde{n}_\tau)$

*Step 2: Minimize conformance cost*

- 11:  $\{\ell_1, \dots, \ell_{\tilde{n}_\tau}\} \leftarrow 0$
  - 12: **for**  $i = \{1, \dots, \tilde{n}_g\}$  **do**
  - 13:  $\{\tau_1, \dots, \tau_{\tilde{n}_\tau}\} \leftarrow \text{Evolve}((\tau_1, \ell_1), \dots, (\tau_{\tilde{n}_\tau}, \ell_{\tilde{n}_\tau}))$
  - 14: **for**  $j = \{1, \dots, \tilde{n}_\tau\}$  **do**
  - 15: **for**  $D_{T2,l} = \{D_{T2,1}, \dots, D_{T2,n_v}\}$  **do**
  - 16:  $\ell_l \leftarrow (25)$  using  $D_{T2,l}, \tau_j$
  - 17: **end for**
  - 18:  $\ell_j \leftarrow -\sum_{l=1}^{n_v} \ell_l$
  - 19: **end for**
  - 20: **end for**
  - 21:  $\tau^* \leftarrow \text{Best}((\tau_1, \ell_1), \dots, (\tau_{\tilde{n}_\tau}, \ell_{\tilde{n}_\tau}), 1)$
  - 22:  $\alpha^*, \Delta c^* \leftarrow \text{White}(D_C, \tau^*)$
- 

### A. Scalability of the White-Box Identification Approach

For evaluating the scalability of Thm. 2, we simulate a discretized version of a water tank system with uncertain inputs [50], whose dynamics are

$$\begin{aligned} \dot{x}_{t,1} &= u_{t,1} - 0.3\sqrt{x_{t,1}} \\ \dot{x}_{t,i} &= u_{t,i} + 0.3(\sqrt{x^{(i-1)}} - \sqrt{x^{(i)}}), \quad i = 2, \dots, n_x. \end{aligned}$$

The state  $x^{(i)}$  describes the water level of tank  $i$ , such that the system dimension  $n_x$  is equal to the number of tanks, and  $u^{(i)}$  the water flow into tank  $i$ . We assume that there is an inflow in only every third tank,  $u^{(i)} = 0$  for  $i \neq 1, 4, 7, \dots$ , and we measure each state variable, i.e.,  $y^{(i)} = x^{(i)}$  for  $i = 1, \dots, n_y$ . The computation times of the linear program from Thm. 2 using the halfspace constraints from Lemma 2 and the generators constraints from Lemma 3 are presented for a) varying time horizons  $n_k$ , b) a varying number of nominal trajectories  $n_m$ , c) a varying number of sample executions  $n_s$  of each nominal trajectory, and d) a varying measurement dimension  $n_y$ . As we can see from Table I, increasing the number of samples  $n_s$  does not influence the computational complexity of the linear program using the

TABLE I  
COMPUTATION TIMES FOR WHITE-BOX IDENTIFICATION.

$n_k$	$n_m$	$n_s$	$n_y$	Computation time of Thm. 2 [s]	
				Using Lemma 2	Using Lemma 3
4	10	1	3	0.16	<b>0.15</b>
20	10	1	3	16.14	<b>0.83</b>
40	10	1	3	>600.00	<b>1.61</b>
4	100	1	3	0.54	<b>0.26</b>
4	1000	1	3	23.26	<b>2.58</b>
4	10	10	3	<b>0.16</b>	0.18
4	10	100	3	<b>0.16</b>	1.43
4	10	1	6	9.84	<b>0.22</b>
4	10	1	9	>600.00	<b>0.31</b>
4	10	1	100	>600.00	<b>8.53</b>

halfspace constraints since we only consider the sample  $y_a^{(m,s)}$  closest to each halfspace. However, as the halfspace conversion scales exponentially with the dimension of the reachable set [31], halfspace constraints can only be used for systems with small measurement dimension  $n_y$  and small time horizons  $n_k$ . In contrast, using the generator constraints is efficient for high-dimensional systems and long time horizons, but its computational complexity depends substantially on the overall number of measurement trajectories  $n_s \cdot n_m$ .

### B. General Comparison for Different Model Types

We evaluate the proposed identification methods by computing reachset-conformant models for four dynamical systems, which are

- a pedestrian model [40] formulated as the linear state-space model

$$x_{k+1} = \begin{bmatrix} p_1 & 0 & p_2 & 0 \\ 0 & p_1 & 0 & p_2 \\ 0 & 0 & p_1 & 0 \\ 0 & 0 & 0 & p_1 \end{bmatrix} x_k + \begin{bmatrix} p_3 & 0 & 0 & 0 \\ 0 & p_3 & 0 & 0 \\ p_4 & 0 & 0 & 0 \\ 0 & p_4 & 0 & 0 \end{bmatrix} u_k,$$

$$y_k = \begin{bmatrix} 1 & 0 & 0 & 0 \\ 0 & 1 & 0 & 0 \end{bmatrix} x_k + \begin{bmatrix} 0 & 0 & 1 & 0 \\ 0 & 0 & 0 & 1 \end{bmatrix} u_k,$$

where  $p_1 = 1$ ,  $p_2 = 0.01$ ,  $p_3 = 5 \cdot 10^{-5}$ ,  $p_4 = 0.01$ ,

- the pedestrian model converted to an ARX model, using the conversion formulas from [40, Prop. 2], where

$$y_k = \begin{bmatrix} p_1 & 0 \\ 0 & p_1 \end{bmatrix} y_{k-1} + \begin{bmatrix} p_2 & 0 \\ 0 & p_2 \end{bmatrix} y_{k-2}$$

$$+ \begin{bmatrix} 0 & 0 & 1 & 0 \\ 0 & 0 & 0 & 1 \end{bmatrix} u_k + \begin{bmatrix} p_3 & 0 & p_4 & 0 \\ 0 & p_3 & 0 & p_4 \end{bmatrix} u_{k-1}$$

$$+ \begin{bmatrix} p_3 & 0 & 1 & 0 \\ 0 & p_3 & 0 & 1 \end{bmatrix} u_{k-1},$$

with  $p_1 = 2$ ,  $p_2 = -2$ ,  $p_3 = 5 \cdot 10^{-5}$ ,  $p_4 = -1$ ,

- the Lorenz system [51] described by the nonlinear state-space model

$$\dot{x}_t = \begin{bmatrix} (p_1 + u_{t,1})(x_{t,2} - x_{t,1}) \\ (p_2 + u_{t,2})x_{t,1} - x_{t,2} - x_{t,1}x_{t,3} \\ x_{t,1}x_{t,2} - (p_3 + u_{t,3})x_{t,3} \end{bmatrix}$$

$$y_t = \begin{bmatrix} x_{t,1} \\ x_{t,2} \end{bmatrix},$$

with  $p_1 = 10$ ,  $p_2 = 28$ ,  $p_3 = \frac{8}{3}$ ,

- a NARX model, which we call NARX1, whose dynamics are adapted from [52]:

$$y_k = \begin{bmatrix} \frac{y_{k-1,1}}{1 + y_{k-1,2}y_{k-1,2}} + p_1 u_{k-1,1} \\ \frac{y_{k-1,1}y_{k-1,2}}{1 + y_{k-1,2}y_{k-1,2}} + p_2 u_{k-2,2} \end{bmatrix},$$

with  $p_1 = 0.8$ ,  $p_2 = 1.2$ .

The corresponding uncertainty sets  $\mathcal{X}_0$  (only for the state-space models) and  $\mathcal{U}$  are represented by zonotopes with a random center vector with elements between  $-1$  and  $1$  and a random diagonal generator matrix with elements between  $-0.25$  and  $0.25$ .

Using the true model, the true uncertainty sets, and random input trajectories, we simulate 100 conformance test suites  $D_C$  comprising  $n_m = 20$  test cases each. Each test case has a length of  $n_k = n_p + 6$  time steps and contains  $n_s = 10$  measurement trajectories resulting from different uncertainty trajectories, where  $n_p$  is the model order for the ARX and NARX model (we require  $n_p$  measurements for their initialization) and zero for the state-space models if not defined otherwise. More data is required for the black-box identification approach as explained in the respective subsection. The matrices  $G_x$  and  $G_u$  for the uncertainty sets are initialized by identity matrices, and the initial estimates for the unknown parameters and center vectors are sampled from a Gaussian distribution with a standard deviation of 0.01.

We compare the identification methods using the following criteria:

- the *normalized cost*, which is the ratio of the optimal conformance cost  $\ell$  from (25) for the model identified with the considered approach and the conformance cost using the true model and uncertainty sets,
- the *failure rate*, which is the ratio of the number of failure test suites, i.e., test suites where a conformant model could not be identified or where the normalized cost is bigger than 100, to the total number of test suites,
- the *computation time*, which is the time required for solving the conformance problem for one test suite, and
- the root mean squared errors (*RMSE*) between the true parameters and the parameters estimated with the gray-box identification approaches.

In Table II, we present the results averaged over all dynamical systems and non-failure test suites (except for the failure rate) for the proposed identification methods and baseline methods. Given the absence of comparable solutions in the existing literature, we benchmark our methods against baseline approaches derived from our approach but with slight modifications.

As the performance of the identification methods can vary substantially between different test suites and systems, we also visualize the normalized cost as boxplots for all non-failure test suites in Fig. 2. Example test cases, which were not contained in the identification data, with a length of  $n_k = n_p + 10$  time steps, and the reachable sets from the identified models are displayed in Fig. 3. Since the genetic programming approach approximates the Lorenz model with a NARX model, which requires  $n_p = 3$  measurements for

TABLE II  
EVALUATION OF THE PROPOSED IDENTIFICATION METHODS (IN **BOLD**)  
AND BASELINE METHODS.

Approach	Normalized cost	Failure rate [%]	Computation time [s]	RMSE
<b>White</b>	1.00	0	0.09	-
WhiteAdd	1.88	0	0.10	-
<b>GraySeq</b>	1.02	4.00	12.56	0.19
GraySeq2	1.16	0.25	4.95	0.39
GraySim	1.49	11.50	20.67	0.24
<b>BlackCGP</b>	6.53	0.12	219.65	-
BlackGP	12.68	29.57	180.80	-

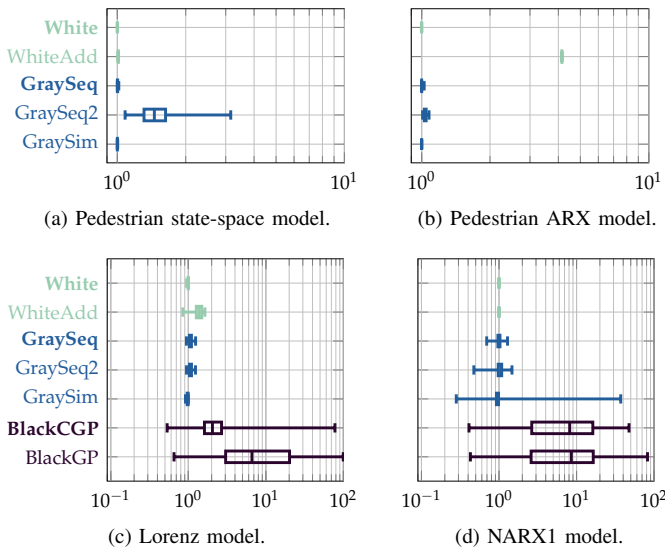


Fig. 2. Normalized cost for the identified models for different non-failure test suites.

its initialization, we enforce that all test cases visualized in Fig. 3c start with the same measurements  $y_i$ ,  $i = 0, \dots, n_p - 1$ , such that we are able to compute one reachable set, which has to enclose all measurements. Thus, we start the reachability predictions at the time step  $k = n_p$  and, to have a fair comparison, we use  $x_{n_p} \oplus \mathcal{X}_0$  as the initial state set, which contains all states of the visualized test cases at  $k = n_p$ , for the nonlinear state-space models identified with the white and gray-box approaches.

1) *White-Box Identification*: We use the linear program in Thm. 2 to identify the white-box models. Please keep in mind that the ARX and NARX models do not require to find  $\alpha_x$  and that  $\Delta c$  is only identified for linear models. We use the halfspace constraints from Lemma 2 instead of the generator constraints from Lemma 3 to shorten computation times, because the considered systems are low-dimensional and the time horizon is short.

We can see from Table II that our identification algorithm, termed *White*, is able to estimate small uncertainty sets, which lead to tight reachable sets, in short computation times. Since the assumed directions for the generators were correct, linear programming is able to find a solution that is as good as using the true uncertainty sets, i.e., the normalized cost in Fig. 2 is always approximately equal to 1. Furthermore, Fig. 3 shows

that the reachable set of the identified model is identical to the reachable set of the true system for the pedestrian state-space model and the pedestrian ARX model. Due to the linearization error, which is not considered in the identification but added for the computation of the reachable set, *White* identifies more conservative uncertainty sets for the nonlinear models, resulting in larger reachable sets after longer time horizons (see Fig. 3d at  $k = n_p + 9$ ). The magnitude of the conservatism depends on the degree of the nonlinearities of the model.

Given that previous research focused only on additive uncertainty sets [26], [29], we use an identification approach based on Thm. 2 that considers only additive measurement error sets in the optimization, termed *WhiteAdd*, as our baseline method. The performance of *WhiteAdd* compared to *White* depends on how well additive uncertainties can approximate the uncertainties of the true systems. The true uncertainties of the pedestrian state-space model and the NARX1 model have a similar influence as additive uncertainties. As a result, the normalized cost of the models identified with *WhiteAdd* is almost identical to the cost of the models identified with *White* for these systems (see Figs. 2a and 2d). However, the true uncertainties of the pedestrian ARX model and Lorenz model have a more complex influence on the system, which cannot be well approximated by additive uncertainties. This can lead to bigger uncertainty sets and reachable sets (see Figs. 3b and 3c) and, thus, higher normalized costs (see Figs. 2b and 2c). In some cases, we even obtain models that are not reachset-conformant for validation test cases (see Fig. 3c, where the measurements are not contained in the reachable sets  $\mathcal{Y}^{\text{WhiteAdd}}$  at  $k = n_p + 9$ ).

If we know how the uncertainties act on the system, we should use this knowledge in the identification by applying the proposed algorithm *White*. The computation times are very short, and the identification results are always as good as or better than those of an identification algorithm that only considers additive uncertainty sets.

2) *Gray-Box Identification*: We evaluate the gray-box identification approaches from Sec. V by augmenting the identification variables from the previous subsection with the model parameters  $p$ . Furthermore, we assume that the center vector of the uncertainty set of the NARX1 model is unknown, such that  $c_u$  is added to the identification variables for this model.

As we can see from Fig. 2, the proposed sequential approach, termed *GraySeq*, yields the smallest cost values for the linear models and the NARX1 model of all gray-box identification approaches, while the simultaneous identification approach from [41], *GraySim*, results in marginally smaller cost values than *GraySeq* for the Lorenz model. Furthermore, we evaluate another sequential identification approach, called *GraySeq2*, where we replace the cost function  $\ell_U$  from (26) with the least-squares cost function  $\ell_{LS}$  from (27). This approach leads to the shortest computation times but also higher normalized costs and bigger reachable sets (see Table II and Figs. 2 and 3). As displayed in Table II, all three identification methods lead to small root mean squared errors between the estimated parameters and the true parameters, where *GraySeq* shows the smallest error on average. *GraySim* has the highest failure rate due to the NLP solver converging

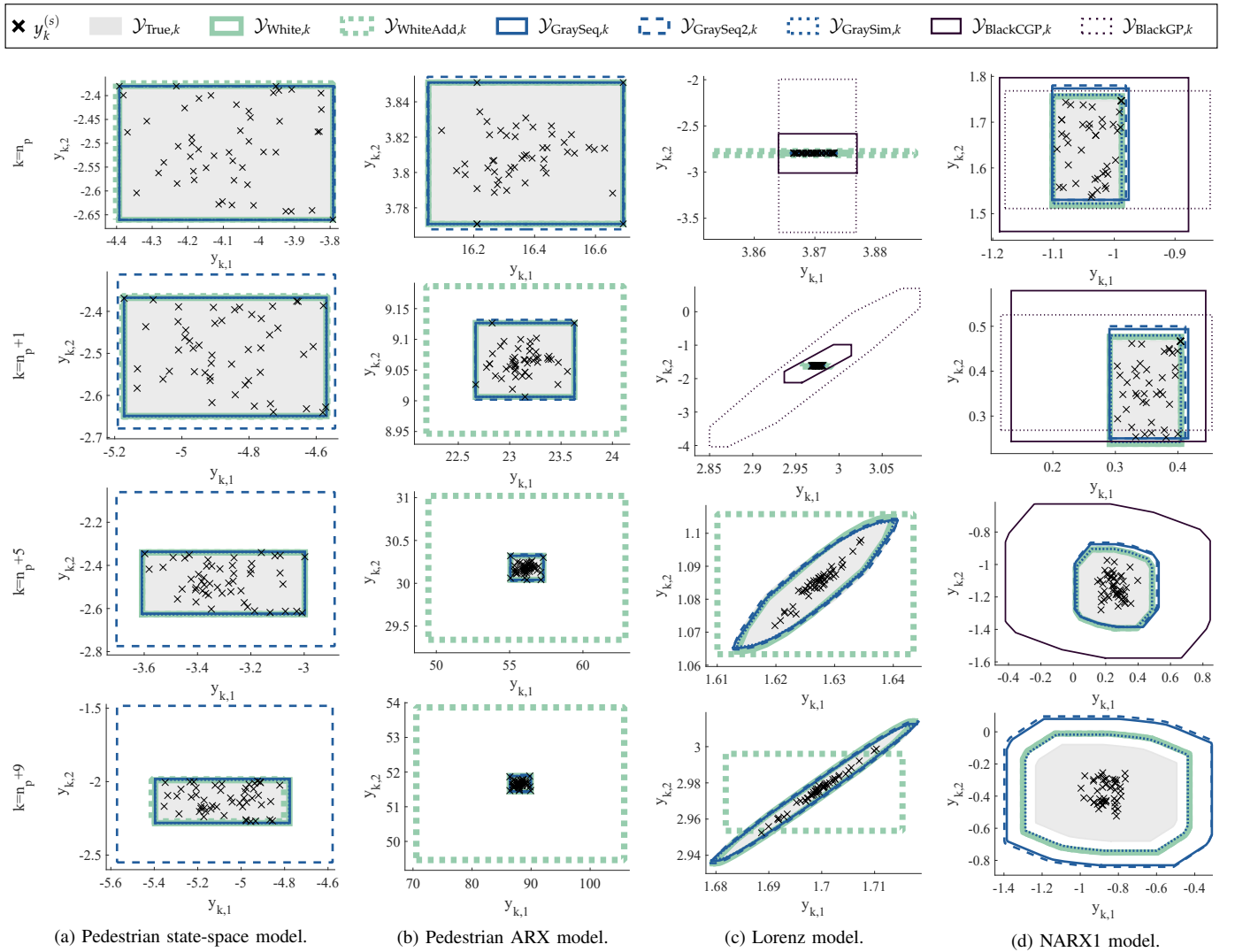


Fig. 3. Example test cases: measurements  $y_k^{(s)}$ , reachable set  $\mathcal{Y}_{\text{true},k}$  of the true system, and reachable sets  $\mathcal{Y}_{\text{method},k}$  from models identified with different white, gray, and black-box identification methods for the time steps  $k = n_p, n_p + 1, n_p + 5, n_p + 9$ .

to local optima.

**3) Black-Box Identification:** Lastly, we test the black-box identification approaches. As the model structure of linear models is completely determined by the linearity and the system dimension, which could be estimated by comparing the gray-box identification results for different dimensions, we only apply our black-box identification approaches to the two nonlinear systems.

First, we generate an additional training dataset consisting of 1500 test cases for step 1 of Alg. 3 and 100 test cases for step 2. Each test case contains the measurements resulting from  $n_s = 10$  uncertainty trajectories with a length of  $n_k = n_p + 6$  time steps. For the model order, we choose  $n_p = 3$  for approximating the Lorenz model and  $n_p = 2$  for the NARX1 model. The accuracy of our black-box identification approach can be improved by using more complex models and more identification data. As such improvements always involve a trade-off in computation time, the decision will depend on the accuracy required for the application.

Next, we evolve a model population with genetic pro-

gramming, using functionalities from the MATLAB toolbox GPTIPS2 [48]. The standard genetic programming algorithm, termed *BlackGP*, aims to minimize the least-squares cost function in (27) for the training data over 100 generations for a population of 300 randomly initialized models. From the final population, we choose the model with the highest fit to the data. Additionally, we evaluate the conformant genetic programming approach, denoted as *BlackCGP*, where we minimize the least-squares cost function over  $n_g = 95$  generations for  $n_\tau = 300$  models, followed by  $\tilde{n}_g = 5$  generations, where the conformance cost from (25) is minimized for  $\tilde{n}_\tau = 100$  models.

As the considered identification methods are of stochastic origin, the data generation and black-box identification process is repeated 30 times. The normalized cost for all test suites is displayed in the boxplots in Fig. 2 for the final models from all genetic programming runs.

While both approaches lead to similar normalized costs for the NARX1 model (see Fig. 2d), the costs for identifying the Lorenz system with *BlackCGP* are much smaller (see

Fig. 2c). This is also shown in Figs. 3c and 3d (we do not display the reachable sets  $\mathcal{Y}_{\text{BlackCGP},k}$  and  $\mathcal{Y}_{\text{BlackGP},k}$  at the time steps  $k = n_p + 5$  and  $k = n_p + 9$  if they are too big): The models identified with *BlackCGP* mimic the reachability of the true system well in an overapproximative way. In contrast, the results of *BlackGP* are more volatile. The models identified with *BlackCGP* mimic the reachability of the true system well in an overapproximative way. In contrast, the results of *BlackGP* are more volatile. The identified Lorenz model depicted in Fig. 3c leads to more conservative reachable sets, while the reachable set of the identified NARX model depicted in Fig. 3d is too small, as it does not contain all validation measurements at time step  $k = n_p + 1$ . Furthermore, as can be seen from Table II, the models identified with *BlackGP* lead more often to failures in the conformance identification step. These failures result partially from exploding reachable sets when considering set-based inputs and partially from an insufficient influence of the input on the model dynamics, i.e., by increasing the scaling factors of the input set, we are not able to enlarge the reachable set in all dimensions, especially at early time steps, such that not all measurements can be enclosed and the model cannot be made reachset-conformant.

### C. Identification of a Vehicle Model

Finally, we test our identification method with measurements of the automated vehicle EDGAR [53], which is depicted in Fig. 1. Given the limited number of available test cases, we only validate our white-box and gray-box identification methods. We use the following kinematic model [54]:

$$\begin{aligned} \dot{x}_t &= \begin{bmatrix} x_{t,4} \cos(\beta + x_{t,5}) \\ x_{t,4} \sin(\beta + x_{t,5}) \\ r_\delta u_{t,1} \\ u_{t,2} \\ x_{t,4} \cos(\beta) \frac{\tan(x_{t,3})}{l} \end{bmatrix} + u_{t,3:7} \\ y_t &= \begin{bmatrix} x_{t,1} \\ x_{t,2} \\ \frac{1}{r_\delta} x_{t,3} \\ x_{t,4} \end{bmatrix} + u_{t,8:11}, \end{aligned}$$

where the slip angle  $\beta$  can be computed as

$$\beta = \arctan\left(\tan(x_{t,3}) \frac{l_r}{l}\right).$$

The state vector  $x_t = [p_{x,t} \ p_{y,t} \ \delta_{f,t} \ v_t \ \psi_t]^\top$  consists of the position in  $x$  and  $y$  direction, the steering angle at the front axle, the vehicle velocity, and the yaw angle, respectively. We obtain noisy measurements of the position,  $y_{t,1} = \hat{p}_{x,t}$  and  $y_{t,2} = \hat{p}_{y,t}$ , the steering wheel angle  $y_{t,3} = \hat{\delta}_{s,t}$ , and the velocity  $y_{t,4} = \hat{v}_t$ . The input and disturbance vector  $u_t = [\hat{\delta}_{s,t} \ a_{x,t} \ w_t^\top \ v_t^\top]^\top$  is composed of the steering wheel speed  $\hat{\delta}_{s,t}$ , the longitudinal acceleration  $a_{x,t}$ , the process noise vector  $w_t$ , and the measurement noise vector  $v_t$ . The parameters  $r_\delta$ ,  $l$ , and  $l_r$  denote the transmission ratio from  $\delta_s$  to  $\delta_f$ , the wheelbase, and the distance from the front axle to the center of gravity, respectively, and are given for the white-box identification and unknown for the gray-box identification.

The vehicle data is randomly split into an identification and a validation data set. The initial state estimate is computed

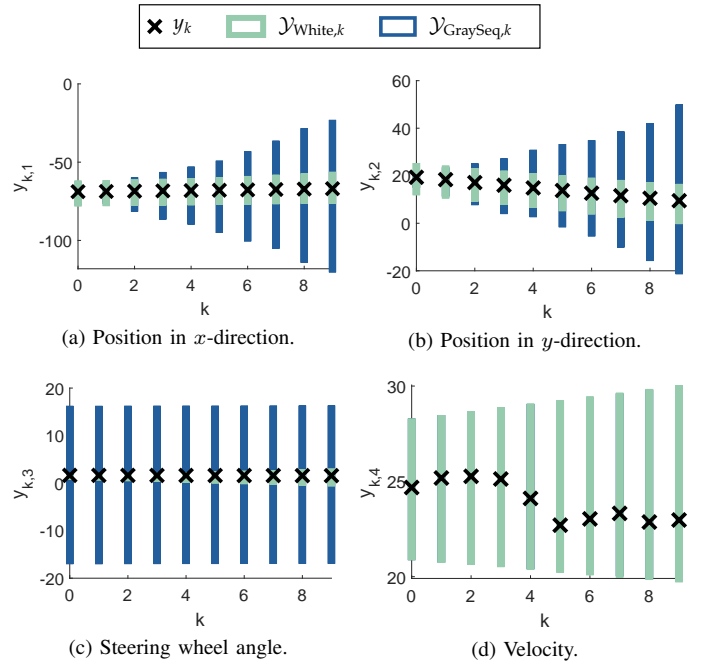


Fig. 4. Reachable sets and measurement trajectories for a failure test case of the automated vehicle EDGAR.

from the measurements with  $x_{*0} = [\hat{p}_{x,0} \ \hat{p}_{y,0} \ r_\delta \hat{\delta}_{s,0} \ \hat{v}_0 \ \hat{\psi}_0]^\top$  where the initial yaw angle is calculated as

$$\hat{\psi}_0 = \arctan\left(\frac{\hat{p}_{y,1} - \hat{p}_{y,0}}{\hat{p}_{x,1} - \hat{p}_{x,0}}\right).$$

From the  $n_m = 84$  test cases of the identification data set with a length of  $n_k = 6$  time steps and  $n_s = 1$ , we identify the following uncertainty sets with the white-box identification approach from Thm. 2:

$$\begin{aligned} \hat{\mathcal{X}}_0 &= \langle \mathbf{0}, \text{diag}([0.00 \ 0.55 \ 0.00 \ 0.66 \ 0.00]) \rangle, \\ \hat{\mathcal{U}}_{in} &= \langle \mathbf{0}, \text{diag}([0.00 \ 0.00]) \rangle, \\ \hat{\mathcal{W}} &= \langle \mathbf{0}, \text{diag}([0.03 \ 0.02 \ 0.00 \ 0.06 \ 0.00]) \rangle, \\ \hat{\mathcal{V}} &= \langle \mathbf{0}, \text{diag}([2.82 \ 1.84 \ 0.05 \ 0.79]) \rangle, \end{aligned}$$

with  $\hat{\mathcal{U}}_c = \hat{\mathcal{U}}_{in} \times \hat{\mathcal{W}} \times \hat{\mathcal{V}}$ . The large values in  $\hat{\mathcal{V}}$  indicate a large measurement uncertainty. The sequential gray-box identification approach *GraySeq* also leads to larger initial state and process noise uncertainties, while identifying small non-zero center vectors for all uncertainties.

Next, we validate these results by computing the reachable sets for the  $n_m = 304$  test cases of the validation data set with a length of  $n_k = 10$  time steps. 98.9% of the measurements are contained in their corresponding reachable set for the white-box model and 93.6% for the gray-box model, which shows that the proposed identification framework works well for real-world data. One of the failure cases is presented in Fig. 4. We can see in Fig. 4d that the measurement at time 0.25s is marginally outside the reachable set (the reachable velocities are identical for both models for this test case). Introducing safety factors for scaling the identified uncertainty sets decreases the failure rate, i.e., a safety factor of  $\epsilon = 1.2$  leads to 99.2% contained measurements for the white-box model and 97.6% for the gray-box model, while

all measurements are contained in the respective reachable sets for both models when using a safety factor of  $\epsilon = 3$ . The magnitude of the necessary safety factor shows that the data contains some outliers (measurements that deviate substantially from the expected outputs). Thus, a lower failure rate could also be achieved by detecting and removing outliers from the measurement data.

## VIII. CONCLUSIONS

We introduce a novel framework for identifying reachset-conformant models for linear and nonlinear system dynamics, accommodating different levels of prior knowledge. A key innovation is the usage of the GO model, which unifies reachability analysis for many model types. Building on this model, we present the first reachset-conformant identification method capable of handling potentially non-additive uncertainty sets and input-output models. Our framework also extends to the estimation of unknown model parameters and the identification of reachset-conformant black-box models using genetic programming, allowing for modeling complex systems with minimal prior information. Through extensive numerical experiments involving the identification of linear state-space, ARX, nonlinear state-space, and NARX models, as well as the modeling of an automated vehicle using real-world data, we demonstrate the robustness and practical applicability of our proposed approaches. In all experiments, we are able to identify reachset-conformant models, whose reachable sets tightly enclose all measurements, in competitive computation times.

In summary, our work offers a versatile and robust framework for reachset-conformant system identification from data. The reachset conformance property ensures that the identified models are applicable in formal verification and control of real-world systems, promising enhanced reliability and reduced conservatism in practical applications. Therefore, this novel framework fills a critical gap in current methodologies.

## REFERENCES

- [1] H. Roehm, J. Oehlerking, M. Woehle, and M. Althoff, "Model conformance for cyber-physical systems: A survey," *ACM Transactions on Cyber-Physical Systems*, vol. 3, no. 3, 2019. article no. 30.
- [2] L. Ljung, *System Identification: Theory for the User*. Prentice Hall, 1999.
- [3] R. Isermann and M. Münchhof, *Identification of Dynamic Systems*. Springer, 2011.
- [4] K. J. Keesman, *System Identification: An Introduction*. Springer, 2011.
- [5] R. Tóth, *Modeling and Identification of Linear Parameter-Varying Systems*. Springer, 2010.
- [6] B. T. Polyak, S. A. Nazin, C. Durieu, and E. Walter, "Ellipsoidal parameter or state estimation under model uncertainty," *Automatica*, vol. 40, no. 7, pp. 1171–1179, 2004.
- [7] M. Canale, L. Fagiano, and M. Signorile, "Design of robust predictive control laws using set membership identified models," *Asian Journal of Control*, vol. 15, no. 6, pp. 1714–1722, 2013.
- [8] E. Walter and H. Piet-Lahanier, "Estimation of parameter bounds from bounded-error data: A survey," *Mathematics and Computers in Simulation*, vol. 32, no. 5-6, pp. 449–468, 1990.
- [9] M. Kieffer, E. Walter, and I. Simeonov, "Guaranteed nonlinear parameter estimation for continuous-time dynamical models," *IFAC Proceedings Volumes*, vol. 39, no. 1, pp. 843–848, 2006.
- [10] B. T. Polyak and S. A. Nazin, "Interval parameter estimation under model uncertainty," *IFAC Proceedings Volumes*, vol. 38, no. 1, pp. 118–123, 2005.
- [11] M. Casini, A. Garulli, and A. Vicino, "Feasible parameter set approximation for linear models with bounded uncertain regressors," *IEEE Transactions on Automatic Control*, vol. 59, no. 11, pp. 2910–2920, 2014.
- [12] J. Bravo, T. Alamo, and E. Camacho, "Bounded error identification of systems with time-varying parameters," *IEEE Transactions on Automatic Control*, vol. 51, no. 7, pp. 1144–1150, 2006.
- [13] A. Rauh, J. Kersten, and H. Aschemann, "Interval methods and contractor-based branch-and-bound procedures for verified parameter identification of quasi-linear cooperative system models," *Journal of Computational and Applied Mathematics*, vol. 367, pp. 1–10, 2019.
- [14] N. R. Mahato, L. Jaulin, S. Chakraverty, and J. Dezert, "Validated enclosure of uncertain nonlinear equations using SIVIA Monte Carlo," in *Recent Trends in Wave Mechanics and Vibrations*, pp. 455–468, Springer, 2020.
- [15] M. Kieffer and E. Walter, "Guaranteed estimation of the parameters of nonlinear continuous-time models: Contributions of interval analysis," *International Journal of Adaptive Control and Signal Processing*, vol. 25, no. 3, pp. 191–207, 2011.
- [16] S. H. Mo and J. P. Norton, "Fast and robust algorithm to compute exact polytope parameter bounds," *Mathematics and Computers in Simulation*, vol. 32, no. 5-6, pp. 481–493, 1990.
- [17] A. Alanwar, A. Koch, F. Allgöwer, and K. H. Johansson, "Data-driven reachability analysis using matrix zonotopes," in *Proceedings of the 3rd Conference on Learning for Dynamics and Control*, vol. 144, pp. 163–175, 2021.
- [18] Y. Chen and N. Ozay, "Data-driven computation of robust control invariant sets with concurrent model selection," *IEEE Transactions on Control Systems Technology*, vol. 30, no. 2, pp. 495–506, 2022.
- [19] S. Sadraddini and C. Belta, "Formal guarantees in data-driven model identification and control synthesis," in *Proc. of the 21st ACM International Conference on Hybrid Systems: Computation and Control*, pp. 147–156, 2018.
- [20] S. K. Mulagaleti, A. Bemporad, and M. Zanon, "Data-driven synthesis of robust invariant sets and controllers," *IEEE Control Systems Letters*, vol. 6, pp. 1676–1681, 2022.
- [21] A. El-Guindy, D. Han, and M. Althoff, "Formal analysis of drum-boiler units to maximize the load-following capabilities of power plants," *IEEE Transactions on Power Systems*, vol. 31, no. 6, pp. 4691–4702, 2016.
- [22] B. Schürmann, D. Heß, J. Eilbrecht, O. Stursberg, F. Köster, and M. Althoff, "Ensuring drivability of planned motions using formal methods," in *Proc. of the IEEE International Conference on Intelligent Transportation Systems*, pp. 1–8, 2017.
- [23] N. Kochdumper and S. Bak, "Conformant synthesis for Koopman operator linearized control systems," in *2022 IEEE 61st Conference on Decision and Control (CDC)*, pp. 7327–7332, 2022.
- [24] M. Althoff, A. Giusti, S. B. Liu, and A. Pereira, "Effortless creation of safe robots from modules through self-programming and self-verification," *Science Robotics*, vol. 4, no. 31, p. eaaw1924, 2019.
- [25] L. Schäfer, F. Gruber, and M. Althoff, "Scalable computation of robust control invariant sets of nonlinear systems," *IEEE Transactions on Automatic Control*, vol. 69, no. 2, pp. 755–770, 2024.
- [26] M. Althoff and J. M. Dolan, "Reachability computation of low-order models for the safety verification of high-order road vehicle models," in *American Control Conference*, pp. 3559–3566, 2012.
- [27] N. Kochdumper, A. Tarraf, M. Rechmal, M. Olbrich, L. Hedrich, and M. Althoff, "Establishing reachset conformance for the formal analysis of analog circuits," in *Proc. of the 25th Asia and South Pacific Design Automation Conference*, pp. 199–204, 2020.
- [28] F. Gruber and M. Althoff, "Scalable robust safety filter with unknown disturbance set," *IEEE Transactions on Automatic Control*, vol. 68, no. 12, pp. 7756–7770, 2023.
- [29] S. B. Liu, B. Schürmann, and M. Althoff, "Guarantees for real robotic systems: Unifying formal controller synthesis and reachset-conformant identification," *IEEE Transactions on Robotics*, vol. 39, no. 5, pp. 3776–3790, 2023.
- [30] M. Althoff, "Checking and establishing reachset conformance in CORA 2023," in *Proc. of the Workshop on Applied Verification of Continuous and Hybrid Systems*, pp. 9–33, 2023.
- [31] L. Lützwow and M. Althoff, "Scalable reachset-conformant identification of linear systems," *IEEE Control Systems Letters*, vol. 8, pp. 520–525, 2024.
- [32] A. Girard, "Reachability of uncertain linear systems using zonotopes," in *Proc. of the 8th ACM International Conference on Hybrid Systems: Computation and Control*, pp. 291–305, 2005.
- [33] W. Kühn, "Rigorously computed orbits of dynamical systems without the wrapping effect," *Computing*, vol. 61, no. 1, pp. 47–67, 1998.

- [34] M. Althoff, O. Stursberg, and M. Buss, “Computing reachable sets of hybrid systems using a combination of zonotopes and polytopes,” *Nonlinear Analysis: Hybrid Systems*, vol. 4, no. 2, pp. 233–249, 2010.
- [35] A. Platzer and E. M. Clarke, “The image computation problem in hybrid systems model checking,” in *Hybrid Systems: Computation and Control*, pp. 473–486, 2007.
- [36] T. Gan, M. Chen, Y. Li, B. Xia, and N. Zhan, “Reachability analysis for solvable dynamical systems,” *IEEE Transactions on Automatic Control*, vol. 63, no. 7, pp. 2003–2018, 2018.
- [37] L. Jaulin, M. Kieffer, and O. Didrit, *Applied Interval Analysis*. Springer, 2006.
- [38] M. Althoff, “Reachability analysis of nonlinear systems using conservative polynomialization and non-convex sets,” in *Proc. of the 16th ACM International Conference on Hybrid Systems: Computation and Control*, pp. 173–182, 2013.
- [39] M. Althoff and J. J. Rath, “Comparison of guaranteed state estimators for linear time-invariant systems,” *Automatica*, vol. 130, 2021. article no. 109662.
- [40] L. Lützwow and M. Althoff, “Reachability analysis of ARMAX models,” in *Proc. of the 62nd IEEE Conference on Decision and Control*, pp. 7021–7028, 2023.
- [41] S. B. Liu and M. Althoff, “Online verification of impact-force-limiting control for physical human-robot interaction,” in *Proc. of the IEEE/RSJ International Conference on Intelligent Robots and Systems*, pp. 777–783, 2021.
- [42] N. Mohajerin and S. L. Waslander, “Multistep prediction of dynamic systems with recurrent neural networks,” *IEEE Transactions on Neural Networks and Learning Systems*, vol. 30, no. 11, pp. 3370–3383, 2019.
- [43] O. Nelles and R. Isermann, “Basis function networks for interpolation of local linear models,” in *Proceedings of 35th IEEE Conference on Decision and Control*, vol. 1, pp. 470–475 vol.1, 1996.
- [44] J. A. K. Suykens, B. L. R. De Moor, and J. Vandewalle, “Nonlinear system identification using neural state space models, applicable to robust control design,” *International Journal of Control*, vol. 62, no. 1, pp. 129–152, 1995.
- [45] J. Sjöberg, Q. Zhang, L. Ljung, A. Benveniste, B. Delyon, P.-Y. Glorennec, H. Hjalmarsson, and A. Juditsky, “Nonlinear black-box modeling in system identification: A unified overview,” *Automatica*, vol. 31, no. 12, pp. 1691–1724, 1995.
- [46] J. R. Koza, “Genetic programming as a means for programming computers by natural selection,” *Statistics and Computing*, vol. 4, no. 2, pp. 87–112, 1994.
- [47] J. Madár, J. Abonyi, and F. Szeifert, “Genetic programming for the identification of nonlinear input-output models,” *Industrial & Engineering Chemistry Research*, vol. 44, no. 9, pp. 3178–3186, 2005.
- [48] D. P. Seanson, *GPTIPS 2: An Open-Source Software Platform for Symbolic Data Mining*, pp. 551–573. Springer, 2015.
- [49] M. Althoff, “An introduction to CORA 2015,” in *Proc. of the Workshop on Applied Verification for Continuous and Hybrid Systems*, pp. 120–151, 2015.
- [50] M. Althoff, O. Stursberg, and M. Buss, “Reachability analysis of nonlinear systems with uncertain parameters using conservative linearization,” in *Proc. of the 47th IEEE Conference on Decision and Control*, pp. 4042–4048, 2008.
- [51] E. N. Lorenz, “Deterministic nonperiodic flow,” *Journal of Atmospheric Sciences*, vol. 20, no. 2, pp. 130 – 141, 1963.
- [52] A. Kroll and H. Schulte, “Benchmark problems for nonlinear system identification and control using soft computing methods: Need and overview,” *Applied Soft Computing*, vol. 25, pp. 496–513, 2014.
- [53] P. Karle, T. Betz, M. Bosk, F. Fent, N. Gehrke, M. Geisslinger, L. Gressenbuch, P. Hafemann, S. Huber, M. Hübner, S. Huch, G. Kaljavesi, T. Kerbl, D. Kulmer, T. Mascetta, S. Maierhofer, F. Pfab, F. Rezabek, E. Rivera, S. Sagmeister, L. Seidlitz, F. Sauerbeck, I. Tahiraj, R. Trauth, N. Uhlemann, G. Würsching, B. Zarrouki, M. Althoff, J. Betz, K. Bengler, G. Carle, F. Diermeyer, J. Ott, and M. Lienkamp, “EDGAR: An autonomous driving research platform - from feature development to real-world application,” 2023.
- [54] R. Rajamani, *Lateral Vehicle Dynamics*. Springer, 2012.



**Laura Lützwow** received the Bachelor of Science degree in mechatronics from the Technical University of Ilmenau, Germany, in 2020, and the Master of Science degree in robotics, cognition and intelligence from the Technical University of Munich, Germany, in 2022. In 2022, she was a visiting student researcher at the Massachusetts Institute of Technology, USA. Currently, she is working toward a Ph.D. degree in computer science with the Cyber-Physical Systems Group, School of Computation, Information and Technology, at the Technical University of Munich. Her research interests include system identification, control theory, and reachability analysis, with applications to safety-critical systems.



**Matthias Althoff** (Member, IEEE) received the Diploma Engineering degree in mechanical engineering and the Ph.D. degree in electrical engineering, both from the Technical University of Munich, Germany, in 2005 and 2010, respectively. From 2010 to 2012, he was a Postdoctoral Researcher at Carnegie Mellon University, Pittsburgh, PA, USA, and from 2012 to 2013, he was an Assistant Professor at the Technical University of Ilmenau, Germany. He is currently an Associate Professor in computer science with the Technical University of Munich. His research interests include formal verification of continuous and hybrid systems, reachability analysis, planning algorithms, nonlinear control, robotics, automated vehicles, and power systems.